RESEARCH ARTICLE

Superlattice-based Plasmonic Catalysis: Concentrating Light at the Nanoscale to Drive Efficient Nitrogen-to-Ammonia Fixation at Ambient Conditions

Siew Kheng Boong,[a] Carice Chong,[a] Jinn-Kye Lee,[a] Zhi Zhong Ang,[a] Haitao Li,[b] Hiang Kwee Lee*[a,c]

[a] S. K. Boong, C. Chong, J. K. Lee, Z. Z. Ang, Prof. H. K. Lee
Division of Chemistry and Biological Chemistry, School of Chemistry, Chemical Engineering and Biotechnology
Nanyang Technological University
21 Nanyang Link, Singapore 637371
E-mail: hiangkwee@ntu.edu.sg
[b] Dr. H. L
School of Chemistry and Chemical Engineering
Yangzhou University
Yangzhou, 225002, PR China
[c] Prof. H. K. L
Institute of Materials Research and Engineering
The Agency for Science, Technology and Research (A*STAR)
2 Fusionopolis Way, #08-03, Innovis, 138634, Singapore

Supporting information for this article is given via a link at the end of the document.

Abstract: Plasmonic catalysis promises green ammonia synthesis but is limited by the need of co-catalysts and poor performances due to weak electromagnetic field enhancement. Here, we use two-dimensional plasmonic superlattices with dense electromagnetic hotspots to boost ambient nitrogen-to-ammonia photoconversion without needing co-catalyst. By organizing Ag octahedra into a square superlattice to concentrate light, the ammonia formation is enhanced by ~15-fold and 4-fold over hexagonal superlattice and disorganized array, respectively. Our unique catalyst achieves superior ammonia formation rate and apparent quantum yield up to ~15-fold and ~10^3-fold, respectively, better than traditional designs. Mechanistic investigations reveal the abundance of intense plasmonic hotspots is crucial to promote hot electron generation and transfer for nitrogen reduction. Our work offers valuable insights to design electromagnetically hot plasmonic catalysts for diverse chemical and energy applications.

Introduction

Realizing efficient ammonia production provides a strong impetus for the rapid development of the chemical, agricultural, and energy industries in modern civilization. This is because ammonia is widely used as a nitrogenous precursor in the manufacturing of diverse fertilizer, chemical, and pharmaceutical products, as well as serving as an ideal carbon-free condensed fuel for the deep decarbonization of the global economy.[1] To date, large-scale ammonia production is mainly achieved by reacting hydrogen and nitrogen gases through the Haber-Bosch process. However, this century-old industrial process suffers from poor reaction efficiencies of ~15% and the specific need for extreme reaction conditions (e.g. 773 K and 200 atm) to cleave highly stable N≡N triple bond during the hydrogenation reaction.[2] Together with the use of H_2 gas reformed from fossil fuel as a chemical precursor, the immense energy demand and large carbon footprint render Haber-Bosch reaction unsustainable in the long run.

Enormous research efforts have thus been directed towards greener catalytic approaches (e.g. photocatalysis and electrocatalysis) to realize ammonia synthesis at mild/ambient conditions with the use of water as a viable hydrogen atom source.[1b, 3] Among various emerging strategies for nitrogen fixation, plasmonic catalysis is particularly attractive due to the use of metallic nanoparticles to concentrate light energy directly on catalytic surfaces through the localized surface plasmon resonance (LSPR) effect.[4] This unique light-matter interaction spans across the UV-vis-IR regions, notably allowing facile reaction activation via intriguing plasmonic phenomena such as hot electron transfer and field polarization effects.[5] Till date, plasmonic catalysts for nitrogen fixation mainly comprise of non-shape-controlled noble metal nanoparticles and/or the sparse assemblies of plasmonic building blocks. These plasmonic platforms are usually further integrated with secondary materials (e.g. metal and semiconductor) to improve hot carriers separation/utilization for plasmon-mediated catalysis.[6] However, current approaches still suffer from poor catalytic performances with an apparent quantum yield and ammonia formation rate typically <0.01% and <10 μmol/hr/g, respectively. The performance bottleneck is attributed to the weak electromagnetic field enhancement from (i) the use of isotropic plasmonic nanoparticle and (ii) a lack of effective interparticle plasmonic coupling.[7] While ruthenium co-catalyst can be employed to elevate ammonia formation to ~100 μmol/hr/g, the need for precious metal and sophisticated fabrication protocol impede real-world applications.[8] Addressing these two formidable challenges are important to expedite plasmonic catalysis towards green

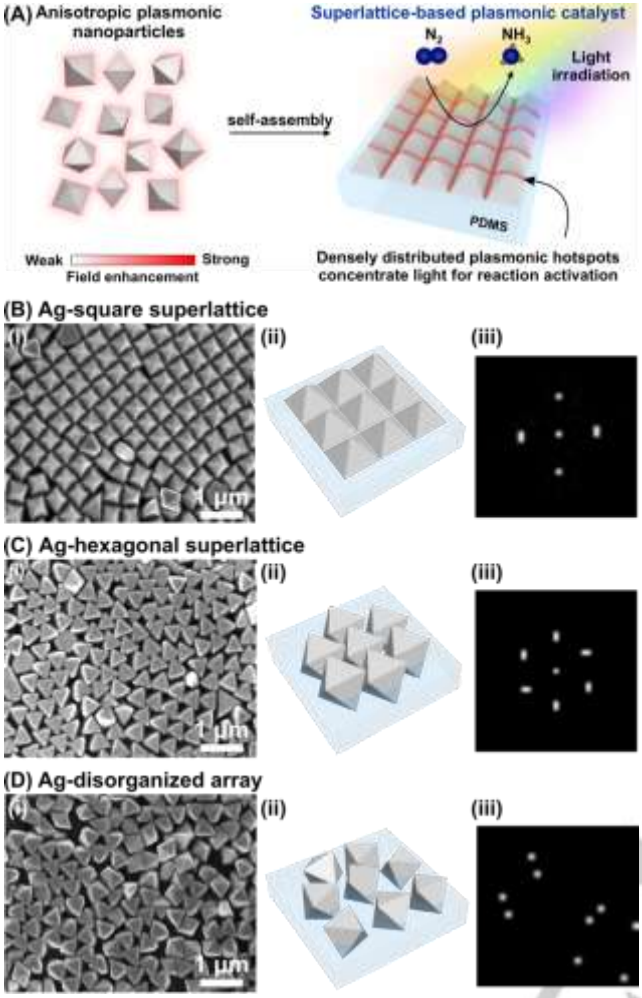

Figure 1. Key concept of plasmonic superlattices for enhanced photocatalytic NRR. (A) Scheme depicting the organization of Ag octahedra into 2D plasmonic superlattice as a superior light-concentrating platform for efficient nitrogen-to-ammonia transformation. (B - D) Ag-square superlattice, Ag-hexagonal superlattice, and Ag-disorganized array, respectively. (i) SEM image, (ii) schematic illustration, and (iii) corresponding fast-Fourier transforms of the SEM image.

ammonia synthesis/utilization using light as a renewable energy source.[9]

Herein, we achieve efficient, plasmon-driven nitrogen-to-ammonia conversion at ideal ambient conditions by organizing plasmonic-active Ag octahedra into close-packed, two-dimensional (2D) superlattices with densely distributed electromagnetic hotspots. Our strategy marries two main concepts to boost plasmonic catalysis (Figure 1A), namely (i) the use of anisotropic plasmonic nanoparticles with strong field confinement at their vertices/edges via the "lightning rod" effect and (ii) the extensive plasmonic coupling between nanoparticles to amplify local electromagnetic field across the catalytic array. Our design aims to tackle the poor field enhancement in current plasmonic catalysis by intensifying electromagnetic hotspots at both the single particle and ensemble levels.

We first demonstrate the organization of Ag building blocks into three distinct 2D assemblies, namely a square superlattice, a hexagonal superlattice, and a disorganized particle array. Optical characterizations of the three plasmonic arrays reveal Ag-square superlattice exhibits the strongest light-concentration ability, notably boosting ammonia production by ~15-fold and 4-fold relative to Ag-hexagonal superlattice and Ag-disorganized array, respectively. Moreover, our unique plasmonic catalyst achieves superior ammonia formation rate and apparent quantum yield up to ~15-fold and ~10^3-fold, respectively, higher than traditional plasmonic/photocatalysts, even without the use of any co-catalyst. Mechanistic studies highlight the high density of plasmonic hotspots generated on Ag-square superlattice is the key to promote hot electron generation and transfer for nitrogen reduction into ammonia. By creating an electromagnetically hot plasmonic ensemble, our unique approach enables better utilization of catalytic materials and light energy to achieve efficient, sustainable light-to-chemical conversion crucial for diverse chemical, environmental, and energy applications.

Results and Discussion

Ag octahedra plays a vital role as an anisotropic building block to create superlattice-based plasmonic catalyst owing to the strong field confinements at its tips/edges.[10] To begin, we synthesize poly(vinylpyrrolidone) (PVP)-capped Ag octahedra with well-defined edges (edge length, 450 ± 17 nm; Figure S1) and vertices via the polyol reduction method.[11] The PVP capping agent on as-synthesized Ag octahedra is then replaced with butanethiol (C_4SH) or dodecanethiol ($C_{12}SH$) to modify its surface chemistry for subsequent self-assembly process.[12] We affirm successful Ag surface modification from the emergence of S 2p XPS peak indexed to the formation of Ag-S bond, as well as the presence of characteristic SERS bands of $C_{12}SH$ ($\upsilon_{C\text{-}C}$, 1085 cm^{-1} and 1130 cm^{-1}) and C_4SH (υ_{CCCC}, 1100 cm^{-1}) after chemical treatment (Figure S2, S3).[13] The chemisorbed $C_{12}SH$ and C_4SH molecules render hydrophobicity to the Ag surfaces, notably attaining a relatively high contact angle of ~137° and 98° (Figure S4), respectively, when compared to the hydrophilic PVP-capped Ag octahedra (contact angle, ~63°). Such facile control over Ag octahedra's surface wetting properties is crucial to direct the formation of different 2D plasmonic arrays with unique optical properties.

The organization of plasmonic building blocks into periodic arrays is necessary to boost both the intensity and density of electromagnetic hotspots for efficient plasmonic catalysis. Thus, we employ a biphasic self-assembly approach to position and orientate the surface-modified Ag octahedra at the water-decane interface, a process driven by the minimization of free energy.[14] The Ag octahedra assemblies are then immobilized on a hydrogel and subsequently transferred onto a polydimethylsiloxane (PDMS; ~2.25 cm^2) support for further characterizations.[15] SEM imaging of the plasmonic arrays shows the formation of three different particle monolayers with unique structural orientations that are pre-defined by their surface chemistry. Hydrophobic $C_{12}SH$-grafted Ag octahedra gives an ordered, square superlattice where particles are standing upright and aligned edge-to-edge (Figure 1B). Hydrophilic PVP-capped Ag octahedra forms a hexagonal close-packed (HCP) superlattice where the building blocks are arranged face-to-face with their neighbouring particles (Figure 1C). C_4SH-modified Ag octahedra with intermediate wetting property assembles into a disorganized particle array (Figure 1D), possibly due to random intermixing of HCP and square configurations. The differences in interfacial

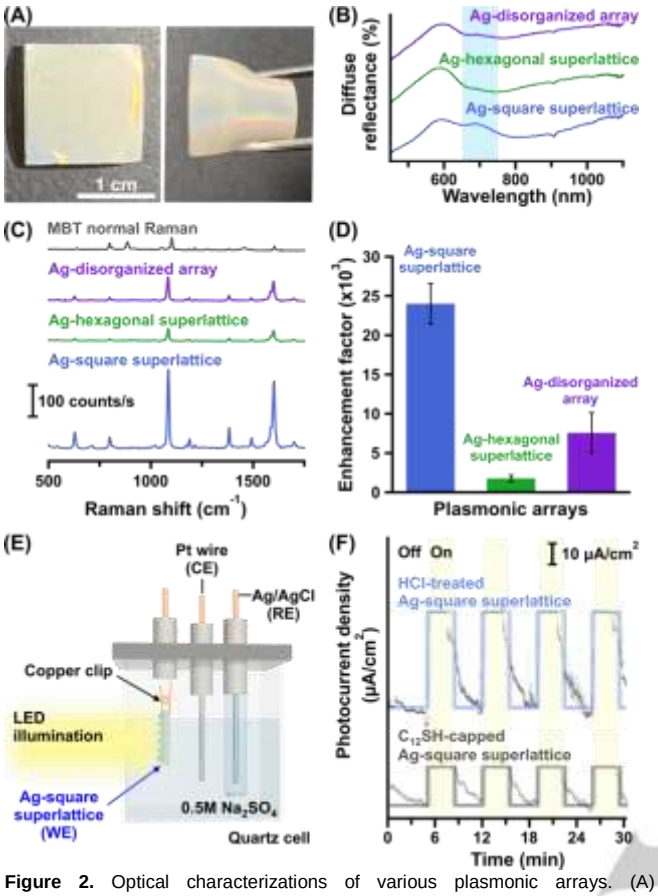

Figure 2. Optical characterizations of various plasmonic arrays. (A) Photographs showing the colour changes upon bending the Ag-square superlattice. (B) Diffuse reflectance spectra and (C) SERS spectra of the three plasmonic Ag arrays. Normal Raman spectrum of 4-methylbenzenethiol (MBT) is included for comparison. (D) Corresponding SERS enhancement factors of the plasmonic arrays. (E) Photoelectrochemical setup for transient photocurrent measurement on the Ag-square superlattice. (F) Photocurrent density of the Ag-square superlattice, with or without HCl treatments, in successive on-off cycles of light irradiation.

behaviour stem from the competition between particle-water, particle-oil, and liquid-liquid interactions. For instance, favourable PVP-water interactions retain hydrophilic Ag octahedra in water to form HCP superlattice, whereas dominant C_{12}SH-oil interactions direct the particles into a standing orientation to optimize their contact with decane while concurrently minimizing the water-decane interface. Fast-Fourier transform analysis of the SEM images identifies the distinct square, hexagonal, and disorganized patterns associated to the respective plasmonic arrays (Figure 1B-D). Hereon, we term the three plasmonic ensembles as Ag-square superlattice, Ag-hexagonal superlattice, and Ag-disorganized array according to their unique structural configurations (Figure S5-S6; Supporting Text 1).

To elucidate critical insights on the structure-to-plasmonic-to-catalytic properties, we first investigate the plasmonic arrays for their (i) localized surface plasmon resonances (LSPR), (ii) plasmonic field enhancement, and (iii) the photogeneration of hot carriers. Understanding these optical properties are important because they are related to light absorption, concentration, and utilization, respectively. We observe obvious superlattice-light interaction from the distinct colour changes when bending the PDMS support, a phenomenon caused by the diffraction and constructive interference of light via angle-dependent Bragg reflection (Figure 2A).[14, 16] Diffuse reflectance spectroscopy (DRS) measurements on the three plasmonic arrays (Figure 2B) display largely similar reflectance spectra with broad features that span across 450 nm – 1100 nm. This observation signifies strong plasmonic superlattice-light interactions in the vis-NIR regions, notably arising from the broadening of LSPRs via the extensive plasmonic couplings within the nanoparticle arrays. More importantly, the Ag-square superlattice exhibits an additional peak at ~700 nm which reflects its enhanced interaction with visible light.

Next, we examine the plasmonic arrays' ability to concentrate light at the nanometre-scale by quantifying plasmonic field enhancements using surface-enhanced Raman spectroscopy (SERS). SERS is used to evaluate field enhancement because the increase in Raman intensity denotes a boost in the plasmonic field and/or chemical effect from molecule-metal complexation.[17] In SERS studies, we first replace the alkylthiol/PVP capping agent on Ag octahedra surfaces with a self-assembled monolayer of 4-methylbenzenethiol (MBT) serving as a SERS reporter. Successful surface modification of Ag surfaces is evident from MBT's characteristic SERS bands at 1085 cm^{-1} (phenyl ring-breathing mode and C-H in plane bending) and 1601cm^{-1} (phenyl stretching; Figure 2C, S7).[14] Using the 1601 cm^{-1} SERS band as a reference, the Ag-square superlattice, Ag-disorganized array and Ag-hexagonal superlattice exhibit an enhancement factor of (2.4×10^4), (7.6×10^3) and (1.8×10^3; Supporting Text 2), respectively. Since all arrays employ the same Ag octahedra and Ag-MBT surface chemistry, any difference in their SERS enhancement factor is thus a measure on the relative plasmonic field strength. Hence, Ag-square superlattice demonstrates the strongest field enhancement which is >3-fold and >13-fold higher than Ag-disorganized array and Ag-hexagonal lattice (Figure 2D), respectively. The superior field enhancement in Ag-square superlattice stems from the extensive edge-to-edge plasmonic coupling between adjacent particles to generate broad strips of intense plasmonic hotspots along Ag octahedra edges (Figure S6).[14] In contrast, Ag-hexagonal superlattice possesses limited hotspots present only at the contacting points between Ag octahedra, whereas Ag-disorganized array has an intermediate field enhancement from random particle-particle contacts. We thus showcase the importance of constructing plasmonic superlattices to boost light-matter interactions, even when using the same nanoparticle.

Building on Ag-square superlattice as a superior light-concentrating platform, we further study its ability to generate hot carriers upon plasmon decay by monitoring its transient photocurrent. Notably, photocurrent measurement is a commonly employed technique to quantify hot electron flow.[18] Prior to photocurrent measurement, we replace the long-chain alkylthiol/PVP on plasmonic surfaces with small Cl^- ions to improve hot electron transfer and molecular accessibility to the catalyst surface while preserving its structural integrity (Figure S8-S12). As-treated plasmonic array is also coated with a thin platinum layer (10 nm) to improve electrical conductivity for photocurrent measurement (Figure S13). It is noteworthy that this thin Pt layer is only used in photocurrent measurement but not for subsequent application in photocatalytic NRR. Our photoelectrochemical setup comprises of an argon-saturated Na_2SO_4 electrolyte solution and an Ag-square superlattice working electrode (area, 2.25 cm^2) at an applied potential of -2.5 V (vs. Ag/AgCl; Figure 2E). Upon LED light irradiation, there is a rapid surge in photocurrent generated by the Ag-square

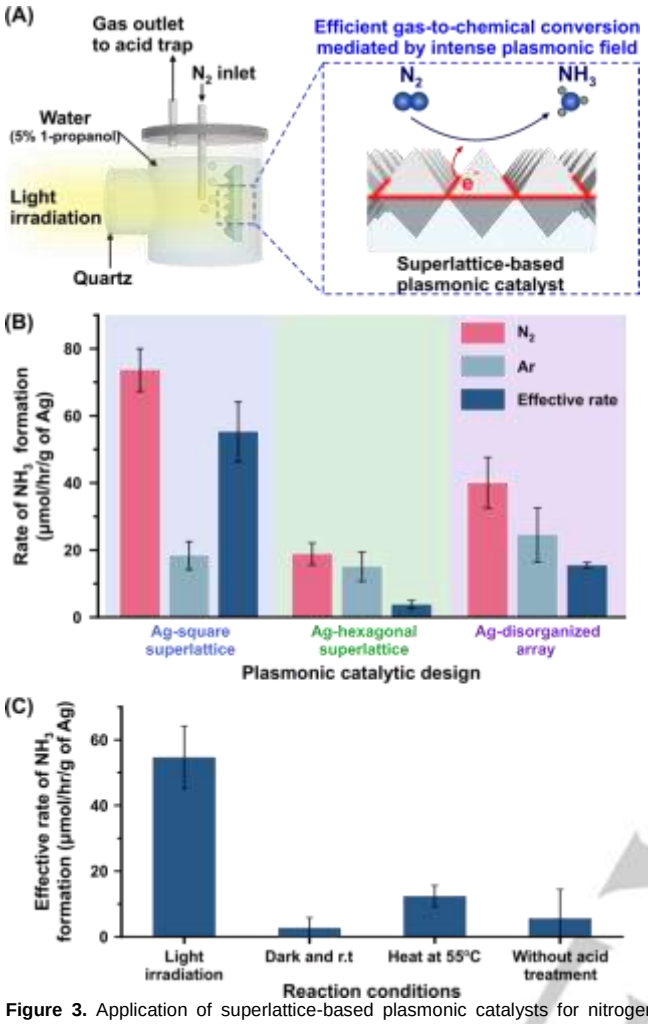

Figure 3. Application of superlattice-based plasmonic catalysts for nitrogen photofixation into ammonia. (A) Scheme illustrating the photoreactor setup for nitrogen reduction using Ag octahedra superlattice as the plasmonic catalyst. (B) Ammonia yield rate of three different plasmonic arrays under white LED illumination and in the presence of N_2 or Ar gas flow. (C) Effective ammonia yield rate obtained using the Ag-square superlattice when subjected to different reaction conditions.

superlattice owing to the generation of plasmon-induced hot carriers. The photocurrent remains relatively stable at ~70 μA/cm^2 under light irradiation, eventually diminishing when the light is switched off (Figure 2F). The on-demand generation of hot carriers is highly reproducible, as demonstrated from the uniform photocurrent (< 2% deviation) recorded over four successive on-off light cycles. Conversely, control C_{12}SH-capped Ag-square superlattice affords low photocurrent (~20 μA/cm^2) which evidently justifies the need to remove alkylthiol from plasmonic surface for efficient hot electron transfer. We exclude potential interference from the Pt coating because of its negligible optical/photocurrent activity (Figure S13C). Our findings jointly point to two key insights, namely (i) hot carriers are indeed produced by the superlattice upon light irradiation and (ii) the plasmon-generated hot electrons can be extracted from the Ag surfaces for chemical reactions.

Having established their ability to generate hot carriers upon light irradiation, we subsequently apply the three Ag nanoparticle arrays as unique plasmonic catalysts to drive nitrogen-to-ammonia conversion at 1 bar and 298 K. Our photocatalytic set-up uses water as a hydrogen atom source and 1-propanol (5% v/v; Figure 3A) as a hole scavenger. Plasmonic catalysis is then initiated and maintained for 2 hr under white LED light irradiation (100 W, Figure S14) with constant N_2 or Ar gas bubbling at 3 sccm. We quantify the ammonia generated using a reported indophenol blue method and a concentration calibration curve (Figure S15; Supporting Text 3). Using Ag-square superlattice as a plasmonic catalyst, we obtain a high rate of NH_3 formation at 73.6 μmol/hr/g under N_2 bubbling. In contrast, a significantly slower rate of 18.4 μmol/hr/g is observed when using Ar bubbling (Figure 3B). By comparing the data obtained under N_2 or Ar bubbling, we determine that Ag-square superlattice achieves an effective ammonia formation rate of 55.3 μmol/hr/g. This is a direct evidence that N_2 gas is indeed the main reactant for ammonia synthesis by eliminating background contributions from remnant dissolved N_2 and/or nitrogen-containing species in the reaction system. We also ascertain the role of 1-propanol as a hole scavenger because control experiment in the absence of propanol leads to slow ammonia formation and obvious chemical degradation of the Ag octahedra (Figure S16). The addition of hole scavenger is thus important to facilitate plasmonic catalysis and avert the self-oxidation of Ag by the hot holes.[19]

More importantly, the Ag-square superlattice exhibits the highest effective rate of ammonia formation (Figure 3B, S17; Supporting Text 4) that is ~15-fold and 4-fold better than Ag-hexagonal superlattice (3.8 μmol/hr/g) and Ag-disorganized array (15.5 μmol/hr/g), respectively. We also note that the trend of effective ammonia formation rate quantitatively matches the relative plasmonic field enhancements of the three plasmonic arrays, whereby Ag-square superlattice > Ag-disorganized array > Ag-hexagonal superlattice. The direct correlation of ammonia formation rate with plasmonic field strength is concrete evidence that concentrating light energy on a plasmonic catalyst is necessary to achieve efficient nitrogen reduction reaction (NRR). It is also noteworthy that Ag-square superlattice contains the lowest particle areal density among the three plasmonic arrays.[14] This observation clearly highlights the importance of organizing plasmonic particles into periodic array to exploit unique plasmonic couplings and intense field enhancement that are otherwise absent in sparsely-distributed and/or random particle systems.

The superior catalytic performance of the Ag-square superlattice potentially originates from three different energy transfer mechanisms, namely (a) hot electron transfer, (b) photothermal heating, and (c) plasmon-induced field polarization. To identify the contributions of each phenomenon to the overall catalytic mechanism, we perform additional control catalytic experiments involving (i) the absence of light at ambient condition, (ii) heating in the dark, and (iii) the use of C_{12}SH-capped Ag-square superlattice as plasmonic catalyst under identical reaction conditions (Figure 3C, S18). First, the application of Ag-square superlattice in dark and at room temperature produces negligible ammonia throughout the reaction (<3 μmol/hr/g), assuring that light energy is the driving force to activate NRR (Figure S19). Second, we infer photothermal heating contributes < 20% to the overall ammonia production rate from the result obtained when Ag-square superlattice is immersed in reaction solution heated at 55 °C in the absence of light. It is noteworthy that macroscopic and nanoscopic temperature measurements reveal that the maximum localized temperature on catalyst surface is at ~55 °C under light irradiation (Figure S20-S22). Third, we examine the contribution from plasmon-induced field polarization by

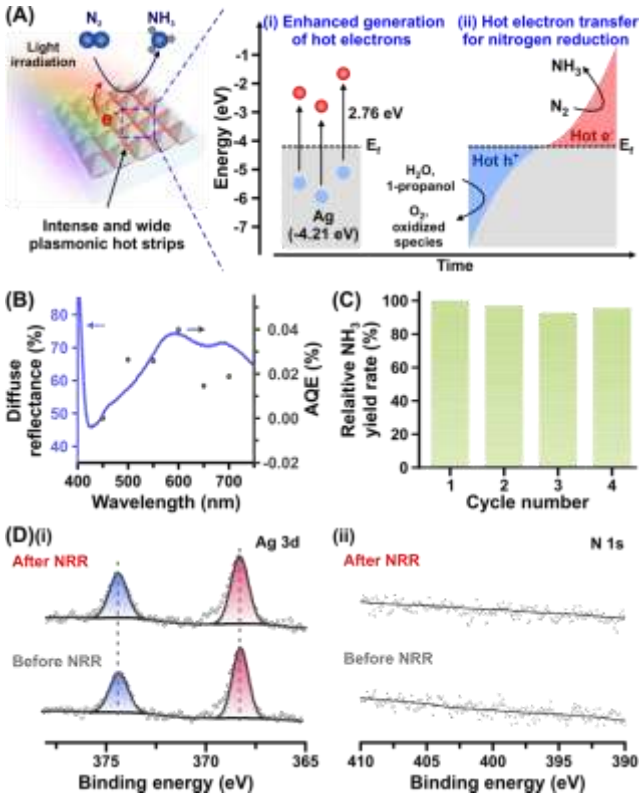

Figure 4. Proposed mechanism and stability of superlattice-based plasmonic catalysis for nitrogen reduction reaction. (A) Scheme illustrating the origin of enhanced NRR when using Ag-square superlattice as the plasmonic catalyst. (B) Co-relation of the diffuse reflectance of Ag-square superlattice with the corresponding apparent quantum efficiencies (AQE) recorded under different monochromatic light irradiation. (C) Ammonia yield rate when using Ag-square superlattice as plasmonic catalyst for four repeated catalytic cycles. (D) High-resolution (i) Ag 3d and (ii) N 1s XPS spectra indicating the chemical stability of Ag-square superlattice after repeated plasmonic catalysis.

comparing with a C_{12}SH-capped Ag-square superlattice because the alkylthiol moieties (length, 1.3 nm) allows N_2 molecules to access the electromagnetic field (<10 nm) but inhibit hot electron transfers.[20] This control plasmonic catalyst exhibits a poor ammonia formation rate (5.6 µmol/hr/g) similar to the reaction in dark and at room temperature, thereby indicating the negligible effect of localized field polarization on NRR.

Collectively, the comprehensive investigations unambiguously highlight that hot electron transfer plays a major role in the superior performance of Ag-square superlattice (Figure 4A). Upon light irradiation, the photoexcitation of Ag octahedra induces the collective oscillation of conduction band electrons, a phenomenon known as the LSPR.[21] Extensive plasmonic couplings between neighbouring particles further amplifies the localized electromagnetic field on the square superlattice by forming wide strips of intense plasmonic hotspots along the nanoparticle edges. Subsequent non-radiative decay of the intense plasmonic field promotes the generation of hot electrons with energies well above Ag's Fermi level (-4.21 eV), as determined by the photon energies (up to 2.76 eV), which are capable of reducing nitrogen. Together with the dense population of plasmonic hotspots over the entire 2D array, our unique superlattice-based plasmonic catalyst essentially boosts the availability and accessibility of hot electrons to the N_2 reactants for their reduction into ammonia. Moreover, hot holes with similar energy level are also generated from the photoexcitation. These hot holes are quenched by their transfer to water or hole scavenger to prevent their accumulation in the superlattice-based plasmonic catalyst. Notably, our Ag-square superlattice is the first catalytic platform built entirely on plasmonic material (e.g. Ag octahedra) and comprise of one-particle thick monolayer. This distinct advantage ensures efficient utilization of light energy and plasmonic building blocks, thereby achieving superior ammonia formation rate and apparent quantum efficiency (AQE; details in next paragraph) up to ~15-fold and ~10^3-fold better than traditional plasmonic/photocatalytic systems that employ additional semiconductor or precious metal as co-catalyst (Table S1).

Moreover, the photocatalytic activity of the superlattice-based plasmonic catalyst can also be precisely modulated by controlling the light irradiation wavelength and power density. When using monochromatic light irradiation at various wavelengths (e.g. 450 nm - 700 nm), we observe the trend of AQE well matches Ag-square superlattice's LSPRs and attains a maximum AQE of 0.04% under 600 nm light excitation (Figure 4B). Furthermore, the systematic rise in light irradiation power density from 68 mW/cm^2 to 213 mW/cm^2 also increases effective ammonia formation rate from 5.3 to 55.3 µmol/hr/g (Figure S23), respectively. The tuneable and direct dependence of catalytic performances on light irradiation wavelength/power clearly assert that the enhanced NRR originates from plasmonic array's strong light-matter interactions and the corresponding plasmon resonances. Our superlattice-based plasmonic catalyst is highly robust and can be easily reused, as evident from the stable ammonia yield rate (<10% deviation) over four successive cycles without the need for intermediate treatment (Figure 4C). Moreover, the Ag-square superlattice also demonstrates excellent structural integrity and chemical stability against potential catalyst poisoning/degradation even with repeated usage (Figure 4D, S24-25).

Conclusion

In conclusion, we have introduced 2D Ag nanoparticle arrays as unique plasmonic catalysts to efficiently valorize naturally abundant nitrogen gas into value-added ammonia at 1 bar and 298 K. Optical characterizations of three distinct plasmonic arrays highlight the importance of organizing Ag octahedra into a square superlattice to boost light-matter interactions and concentrate light directly on catalytic surfaces for facile reaction activation, even without the use of co-catalyst. The Ag-square superlattice notably achieves the best catalytic performance with an effective ammonia yield rate of >53 µmol/h/g, which is ~15-fold and 4-fold higher than Ag-hexagonal superlattice and Ag-disorganized array of the same building block, respectively. More importantly, our superlattice-based plasmonic catalyst enables ammonia production and apparent quantum yield up to ~15-fold and ~10^3-fold, respectively, more superior than conventional photocatalysts and hybrid plasmonic-photocatalytic designs. Systematic investigations into structure-to-plasmonic-to-catalytic properties affirm the generation of intense plasmonic hotspots is the fundamental basis to create energetically hot electrons on the catalyst for nitrogen reduction. Our approach can be extended to a broad range of chemical reactions by incorporating target catalyst onto the plasmonic

superlattices. By intensifying electromagnetic field at the single particle and ensemble levels, we effectively tackle the long-standing challenges in plasmonic catalysis and create enormous opportunities to realize ideal light-to-chemical conversion for green chemical and energy applications.

Acknowledgements

H.K.L. thanks the funding supports from Singapore Ministry of Education (RS13/20 and RG4/21), Agency for Science, Technology and Research, Singapore (A*STAR, A2084c0158), Center of Hydrogen Innovation, National University of Singapore (CHI-P2022-05), and Nanyang Technological University start-up grants. The research was conducted as a part of NICES (NTU-IMRE Chemistry Lab for Eco Sustainability; REQ0275931), a joint research initiative between Nanyang Technological University (NTU) and Institute of Materials Research and Engineering (IMRE) from Agency for Science, Technology and Research (A*STAR).

Keywords: Plasmonic catalysis • Superlattice • Nitrogen fixation • Ammonia generation • Gas-to-fuel/chemical

[1] a) H.-P. Jia, E. A. Quadrelli, *Chem. Soc. Rev.* **2014**, *43*, 547-564; b) X. Xue, R. Chen, C. Yan, P. Zhao, Y. Hu, W. Zhang, S. Yang, Z. Jin, *Nano Res.* **2019**, *12*, 1229-1249; c) V. Rosca, M. Duca, M. T. de Groot, M. T. M. Koper, *Chem. Rev.* **2009**, *109*, 2209-2244; d) D. E. Canfield, A. N. Glazer, P. G. Falkowski, *Science* **2010**, *330*, 192-196.

[2] S. L. Foster, S. I. P. Bakovic, R. D. Duda, S. Maheshwari, R. D. Milton, S. D. Minteer, M. J. Janik, J. N. Renner, L. F. Greenlee, *Nat. Catal.* **2018**, *1*, 490-500.

[3] J. John, D.-K. Lee, U. Sim, *Nano Converg.* **2019**, *6*, 15.

[4] a) U. Aslam, V. G. Rao, S. Chavez, S. Linic, *Nat. Catal.* **2018**, *1*, 656-665; b) M. Dhiman, *J. Mater. Chem. A* **2020**, *8*, 10074-10095; c) Z. Zhang, C. Zhang, H. Zheng, H. Xu, *Acc. Chem. Res.* **2019**, *52*, 2506-2515.

[5] M. Nazemi, M. A. El-Sayed, *Nano Energy* **2019**, *63*, 103886.

[6] X.-C. Ma, Y. Dai, L. Yu, B.-B. Huang, *Light Sci. Appl.* **2016**, *5*, e16017-e16017.

[7] K. Awazu, M. Fujimaki, C. Rockstuhl, J. Tominaga, H. Murakami, Y. Ohki, N. Yoshida, T. Watanabe, *J. Am. Chem. Soc.* **2008**, *130*, 1676-1680.

[8] M. Ali, F. Zhou, K. Chen, C. Kotzur, C. Xiao, L. Bourgeois, X. Zhang, D. R. MacFarlane, *Nat. Commun.* **2016**, *7*, 11335.

[9] a) L. Zhou, D. F. Swearer, C. Zhang, H. Robatjazi, H. Zhao, L. Henderson, L. Dong, P. Christopher, E. A. Carter, P. Nordlander, N. J. Halas, *Science* **2018**, *362*, 69-72; b) J. Wang, J. Heo, C. Chen, A. J. Wilson, P. K. Jain, *Angew. Chem. Int. Ed.* **2020**, *59*, 18430-18434.

[10] a) T. H. Chow, N. Li, X. Bai, X. Zhuo, L. Shao, J. Wang, *Acc. Chem. Res.* **2019**, *52*, 2136-2146; b) S. Gómez-Graña, C. Fernández-López, L. Polavarapu, J.-B. Salmon, J. Leng, I. Pastoriza-Santos, J. Pérez-Juste, *Chem. Mater.* **2015**, *27*, 8310-8317; c) S.-C. Lu, M.-C. Hsiao, M. Yorulmaz, L.-Y. Wang, P.-Y. Yang, S. Link, W.-S. Chang, H.-Y. Tuan, *Chem. Mater.* **2015**, *27*, 8185-8188.

[11] A. Tao, P. Sinsermsuksakul, P. Yang, *Angew. Chem. Int. Ed.* **2006**, *45*, 4597-4601.

[12] a) Q. Yao, Z. Wu, Z. Liu, Y. Lin, X. Yuan, J. Xie, *Chem. Sci.* **2021**, *12*, 99-127; b) M. A. Boles, M. Engel, D. V. Talapin, *Chem. Rev.* **2016**, *116*, 11220-11289; c) A. Castelli, J. de Graaf, S. Marras, R. Brescia, L. Goldoni, L. Manna, M. P. Arciniegas, *Nat. Commun.* **2018**, *9*, 1141.

[13] a) M. A. Bryant, J. E. Pemberton, *J. Am. Chem. Soc.* **1991**, *113*, 8284-8293; b) M. R. Gonçalves, F. Enderle, O. Marti, *J. Nanotechnol.* **2012**, *2012*, 108-122; c) L. Moreno Ostertag, X. Ling, K. F. Domke, S. H. Parekh, M. Valtiner, *Phys. Chem. Chem. Phys.* **2018**, *20*, 11722-11729; d) K. Bian, H. Schunk, D. Ye, A. Hwang, T. S. Luk, R. Li, Z. Wang, H. Fan, *Nat. Commun.* **2018**, *9*, 2365.

[14] Y. H. Lee, W. Shi, H. K. Lee, R. Jiang, I. Y. Phang, Y. Cui, L. Isa, Y. Yang, J. Wang, S. Li, X. Y. Ling, *Nat. Commun.* **2015**, *6*, 6990.

[15] a) T. G. Anjali, M. G. Basavaraj, *J. Colloid Interface Sci.* **2016**, *478*, 63-71; b) T. van de Laar, E. Hooiveld, R. Higler, P. van der Scheer, J. Sprakel, *ACS Nano* **2019**, *13*, 13185-13195.

[16] P. U. P. A. Gilbert, in *Physics in the Arts (Third Edition)* (Ed.: P. U. P. A. Gilbert), Academic Press, **2022**, pp. 169-185.

[17] H. K. Lee, Y. H. Lee, C. S. L. Koh, G. C. Phan-Quang, X. Han, C. L. Lay, H. Y. F. Sim, Y.-C. Kao, Q. An, X. Y. Ling, *Chem. Soc. Rev.* **2019**, *48*, 731-756.

[18] a) Y. Wang, I. Aravind, Z. Cai, L. Shen, G. N. Gibson, J. Chen, B. Wang, H. Shi, B. Song, E. Guignon, N. C. Cady, W. D. Page, A. Pilar, S. B. Cronin, *ACS Appl. Mater. Interfaces.* **2020**, *12*, 17459-17465; b) Y. Park, J. Choi, C. Lee, A.-N. Cho, D. W. Cho, N.-G. Park, H. Ihee, J. Y. Park, *Nano Lett.* **2019**, *19*, 5489-5495.

[19] S. Sheng, Y. Song, L. Sha, K. Ye, K. Zhu, Y. Gao, J. Yan, G. Wang, D. Cao, *Appl. Surf. Sci.* **2021**, *561*, 150080.

[20] O. Sher, Y. Han, H. Xu, H. Li, T. Daun, S. Kumar, A. Grigoriev, P. K. Panda, A. Orthaber, F. Serein-Spirau, T. Jarrosson, S. H. M. Jafri, K. Leifer, *Nanotechnology* **2022**, *33*, 255706.

[21] M. J. Kale, T. Avanesian, P. Christopher, *ACS Catal.* **2014**, *4*, 116-128.

Entry for the Table of Contents

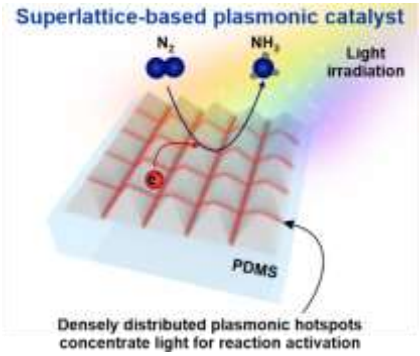

Organizing anisotropic plasmonic nanoparticles into a two-dimensional superlattice is important to intensify the electromagnetic field at both the single-particle and ensemble levels for efficient nitrogen-to-ammonia photoconversion at ambient conditions. Our unique superlattice-based plasmonic catalysts boost the ammonia formation rate and apparent quantum efficiency by up to ~15-fold and ~10^3-fold, respectively, when compared to traditional photocatalytic and hybrid plasmonic-photocatalytic designs.